Results in Physics 15 (2019) 102762

Contents lists available at ScienceDirect

Results in Physics

journal homepage: www.elsevier.com/locate/rinp

# Ab initio calculations of optoelectronic properties of antimony sulfide nano-thin film for solar cell applications

Afiq Radzwan[a,*], Rashid Ahmed[a,b], Amiruddin Shaari[a], Abdullahi Lawal[a,c]

[a] Department of Physics, Faculty of Science, Universiti Teknologi Malaysia, 81310 Skudai, Johor, Malaysia
[b] Centre for High Energy Physics, University of the Punjab, Quaid-e-Azam Campus, 54590 Lahore, Pakistan
[c] Department of Physics, Federal College of Education Zaria, P.M.B 1041, Zaria, Kaduna State, Nigeria

ARTICLE INFO

*Keywords:*
DFT
LAPW
$Sb_2S_3$
Thin-film
Solar cell
Optical properties

ABSTRACT

Antimony sulfide ($Sb_2S_3$) micro thin-film have been received great interest as an absorbing layer for solar cell technology. In this study, to explore its further potential, electronic and optical properties of $Sb_2S_3$ simulated nano-thin film are investigated by the first-principles approach. To do so, the highly accurate full-potential linearized augmented plane wave (FP-LAPW) method framed within density functional theory (DFT) as implemented in the WIEN2k package is employed. The films are simulated in the [0 0 1] direction using the supercell method with a vacuum along z-direction so that slab and periodic images can be treated independently. From our calculations, indirect band gap energy values of $Sb_2S_3$ for various slabs are found to be 0.568, 0.596 and 0.609 eV for 1, 2 and 4 slabs respectively. Moreover, optical properties comprising of real and imaginary parts of the complex dielectric function, absorption coefficient, refractive index are also investigated to understand the optical behavior of the obtained simulated $Sb_2S_3$ thin films. From the analysis of their optical properties, it is clearly seen that $Sb_2S_3$ thin films have good values for optical absorption parameters in the visible and ultraviolet wavelength range, showing the aptness of antimony sulphide thins films for versatile optoelectronic applications as a base material.

## Introduction

The worldwide demand for high performance and low-cost photovoltaic devices is becoming more eminent due to the extensive usage of electricity-consuming devices as a result of the rapid growth of the population [1,2]. The dire requirement for low-cost and efficient optoelectronic devices has led to an increasing focus on a range of different source materials along with the development of a method to characterize these materials [3]. CdTe and Cu(In, Ga)(S, Se) (CIGS) with 30% solar conversion efficiency are leading candidates for light-absorbing materials used in thin-film photovoltaics [4–6]. Nevertheless, the toxicity and restrictions on the usage of Cd being heavy metal and limited supply of In and Te urge for other alternative absorber materials for large-area manufacturing compatibility [7–10], and to reduce the $\$W^{-1}$ price using low-cost materials. To this point, $Sb_2S_3$ semiconductor material has received great attention as a promising candidate for photovoltaic applications, owing to its excellent electronic and optical properties, environmentally friendly constituents, earth-abundant, stable and simple phase with low melting point [2,11–13].

$Sb_2S_3$ is a layered semiconducting material with an orthorhombic crystal structure containing 20 atoms per unit cell [14] and is considered to be useful as an absorbing layer in solar cells because of its potential optical properties [15,16]. The absorption coefficients and optical band gap values of $Sb_2S_3$ macro thin films are reported in the range of $cm^{-1}$ and $1.6 - 1.8eV$ [17,18]. According to an experimental study done by Itzhak et al., the $Sb_2S_3$ thin films that have thicknesses of 10–50 nm have shown great potential for an absorber layer in semiconductor-sensitized solar cell applications [17] due to their high absorption coefficient than other material used in thin-film solar cells. This is one of our motivations to investigate the $Sb_2S_3$ material at nanoscale level [19]. Conversely, the physical properties of nanoscale thin films have also been shown strong dependence on the thickness of the films due to quantum confinement effect or quantum size effects [20,21]. Therefore, investigations, at different length scale, are found in the literature on the thin films of $Sb_2S_3$ to evaluate its impact on the physical properties [22–26].

Tuning of the thickness in semiconductors thin films can lead to changing in their electronic and optical properties due to the confinement of the electrons movement [27]. A recent study on $Sb_2S_3$ thin film, pertaining to the thicknesses from 77 to 206 nm, is reported in the

* Corresponding author at: Department of Physics, Faculty of Science, Universiti Teknologi Malaysia, 81310 Skudai, Johor, Malaysia.
*E-mail addresses:* afiqradzwan1992@gmail.com (A. Radzwan), rashidahmed.pu2@utm.my (R. Ahmed).

https://doi.org/10.1016/j.rinp.2019.102762
Received 2 August 2019; Received in revised form 15 October 2019; Accepted 15 October 2019
Available online 21 October 2019

literature which clearly shows effect of thickness on the optoelectronic properties, indicating the existence of quantum size effect [28]. It is well known that electronic and optical properties of semiconductor materials play an important role in determining their optoelectronic behavior [29].

Usually, density functional theory (DFT) based on GGA and LDA first principles approaches being used for investigating the electronic and optical properties of semiconductor materials [30,31]. First-principles calculations mean an approach of doing calculations that rely on well-established and fundamental laws of science that do not involve any fitting techniques, special models or suppositions. Although GW like methods is also available, they are expensive and impractical for thin-film calculations of semiconductors [32–34].

Here, we use Engel-Vosko approach of exchange correlation potential as it is simple but reproduces usually nice results for optoelectronics properties. Several theoretical works on a thin-film study concerning the effect of thickness for the different materials have been done [35–39], including studies on $Sb_2S_3$ [14,40–44], to the best of our knowledge investigations of electronic and optical properties with highly accurate all-electron full-potential linearized augmented plane wave (FP-LAPW) on $Sb_2S_3$ thin film for different thicknesses, have not been explored yet, due to its complex and disordered structure. In this paper, electronic and optical properties of $Sb_2S_3$ (0 0 1) thin films for different thicknesses were calculated within Engel Vosko generalized gradient approximation (EV-GGA) [45].

## Computational details

Electronic and optical properties of $Sb_2S_3$ thin films with different thicknesses are performed via first-principles full-potential linearized augmented-plane-wave (FP-LAPW) method within the DFT scheme as employed in WIEN2k program [46]. Using slab geometry supercell, the thin films are formed by using optimized lattice constants in (0 0 1) direction using (1 × 1) cell for various thicknesses (1–8 slabs). A slab is represented by optimized bulk of orthorhombic $Sb_2S_3$ ($\alpha = \beta = \gamma = 90^\circ$, a = 1.1646 nm, b = 0.3953 nm and c = 1.1587 nm) as illustrated in Fig. 1. A large vacuum of 3 nm along z-plane was considered to avoid inter-layer interaction.

Table 1 shows a list of thicknesses for different numbers of layers (from 1 to 8 slabs) for $Sb_2S_3$ (0 0 1) thin films. To calculate the total energy of the system, EV-GGA approximation was used as the exchange–correlation potential. The EV-GGA potential has been justified to provide quite accurate band gaps for various semiconducting materials including $Sb_2S_3$ [40,42]. The wave functions are expanded in spherical harmonics inside the Muffin-Tin radius ($R_{MT}$) centered around each nucleus [47]. To ensure the accuracy of the calculations, the $R_{MT}K_{max}$ was set to be 7. Other parameters included in the calculation are used as $G_{max} = 7$ and $I_{max} = 12$, where Gmax is the maximum expansion magnitude of the basis function and $I_{max}$ is the maximum expansion magnitude of the wavefunctions in spherical harmonics inside the muffin tins (MTs). These parameters are selected to determine the extent of the matrix. Three hundred k-points in the first Brillouin zone were adopted in the calculations (250 points in the irreducible part of the surface Brillouin zone). The iterations were stopped when the difference of total energy was less than 0.00001 Ry between the steps, taken as a convergence criterion.

## Results and discussion

### *Electronic properties*

The electronic properties are concerned with band structure calculations and density of states (DOS). For a better understanding of the thickness dependence electronic band structure, we analyze the electronic band structure of $Sb_2S_3$ (0 0 1) film with respect to the number of slabs. The k path selected along high symmetry point in the first Brillouin zone is $Y \rightarrow \Gamma \rightarrow S \rightarrow \Gamma$. The band structure plots of $Sb_2S_3$ in bulk form and film from 1 to 8 slabs with EV-GGA along selected high symmetry directions in the Brillouin zone are presented in Fig. 2. The Fermi energy at the bottom of conduction band is defined to be zero energy (0 eV). EV-GGA functionals are selected in our calculations, it provides good predictions on bandgap value for both bulk and surface states of numerous semiconductor materials than bare GGA [48–50]. Lack of study on 2D materials using this exchange–correlation functional motivated us to use it in our present calculations. It is evident from Fig. 2 that $Sb_2S_3$ slabs exhibit an indirect bandgap with valence band maximum lying between S and Γ and conduction band minimum at Γ-symmetry point respectively. The indirect bandgap value of bulk $Sb_2S_3$ with EV-GGA functionals without spin–orbit coupling was found to be 1.661 eV and this value is in good agreement with previous theoretical work and experimental measurement of 1.1–2.8 eV [13,14,51]. However, our calculated values of indirect energy gaps of $Sb_2S_3$ slabs were found to be 0.568 and 0.596 eV for slab 1 and 2 respectively and this trend is consistent with the experimental work studied by Mane et al. [28] where the bandgap value reduced when the thickness increased. This effect demonstrates the quantum size effect of holes and electrons in $Sb_2S_3$. This change of bandgap becomes evident that thickness of films has an effect on material physical properties. On the other hand, the magnitude of the energy band gap remains the same when the film is more than 3 slabs. Although the energy band gap values are the same when the film thickness is more than 3 slabs the number of bands in both conduction and valence band enhanced as the thickness of $Sb_2S_3$ (0 0 1) films increases and this trend is in quite agreement with previous thin-film studies [52–56]. However, it is clear from Fig. 2 that the indirect energy gap of $Sb_2S_3$ slabs reduced by 1 eV with respect to its bulk counterpart. The reason for lowing bandgap energy in $Sb_2S_3$ films when compared with the bulk form is due to quantum confinement effect that had been discussed in detail and confirmed in various other studies previously [57–60] and our previous study of nanowire [61]. To further probe the nature of the energy gap, we have also studied the total density of states (DOS) of $Sb_2S_3$ films with different slabs within EV-GGA. Fig. 3 shows the graph of total DOS. From the total DOS plots, the peaks of the density of states in the valence band region increase significantly near the Fermi level in number while in the conduction band region the increase starts at 1.5 eV. The increment in total DOS corresponds to the increase in number of atoms and electrons in the films. Therefore, it is possible to exploit the quantum confinement effect to tune the electronic properties in $Sb_2S_3$ films.

### *Optical properties*

This part provides several optical parameters of $Sb_2S_3$ thin films which are determined for the first time by highly accurate first-principles all-electron full-potential linearized augmented plane wave method. Optical parameters of material normally explain the behavior of the material when exposed to electromagnetic radiation and they also help in predicting band structure configuration. The understanding of the optical behavior of material is essential to estimate its usefulness and applicability for optoelectronic applications [62]. Optical behavior is strongly associated with electronic structure [29]. As observed in the electronic band structure analysis, the geometry of the electronic structure for $Sb_2S_3$ thin film changed with film thickness. Several experimental studies have also shown previously that the optical properties of $Sb_2S_3$ thin film are dependent upon the thickness of the film. However, to the best of our knowledge theoretical investigation on $Sb_2S_3$ thin films has not been reported yet on optical properties. In order to describe the said parameters quantitively, it is essential to evaluate dielectric function. Dielectric function is the ratio of the permittivity of a material to the permittivity of free space, whereas permittivity is the measure of the resistance of a material when an electric field is induced in a material. All the dielectric materials are insulator

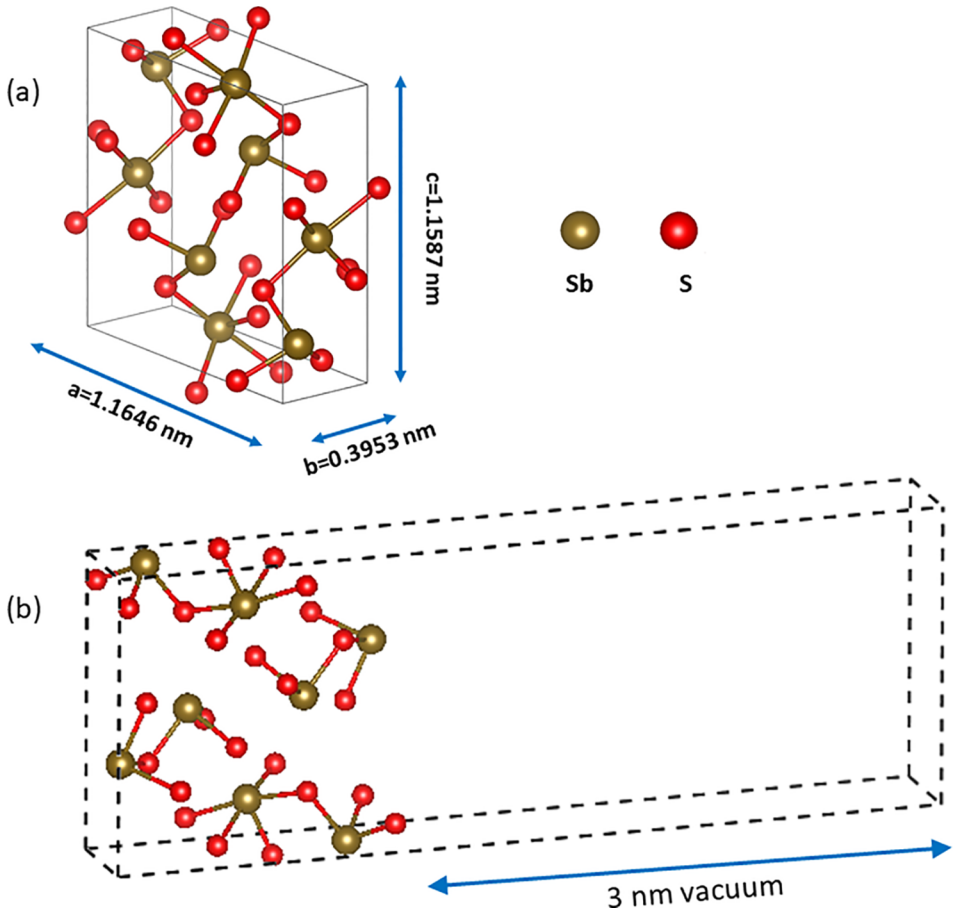


**Fig. 1.** Crystal structure of optimized (a) unit cell of the $Sb_2S_3$ and (b) 1 slab of $Sb_2S_3$ (0 0 1) thin film with 3 nm vacuum.

**Table 1**
Thicknesses for a different number of layers (from 1 to 8 slabs) for $Sb_2S_3$ (0 0 1) thin films.

| Number of slabs | Thickness(nm) |
|---|---|
| 1 | 1.16 |
| 2 | 2.31 |
| 4 | 4.63 |
| 6 | 6.95 |
| 8 | 9.27 |

but all the insulators are not dielectric [63]. The dielectric function consists of real ($\varepsilon_1(\omega)$) and imaginary part ($\varepsilon_2(\omega)$). It is represented as follows:

$$\varepsilon(\omega) = \varepsilon_1(\omega) + i\varepsilon_2(\omega) \quad (1)$$

where $\varepsilon_1(\omega)$ is real part and $\varepsilon_2(\omega)$ is an imaginary part of the dielectric function. Physical properties and band structure rely strongly on $\varepsilon(\omega)$.

As mentioned, we analyzed the optical properties based on EV-GGA functionals. From the knowledge of electronic band structure of a solid, the imaginary part of the dielectric function, $\varepsilon_2(\omega)$ can be calculated from Kubo–Greenwood equation as shown in Eq. (2):

$$\varepsilon_2(\omega) = \frac{2\pi e^2}{\Omega\varepsilon_0} |\langle\psi_k^c|\hat{u} \times \vec{r}|\psi_k^v\rangle| \, \delta(E_k^c - (E_k^v + E)) \quad (2)$$

Once we know the imaginary part, the real part, $\varepsilon_1(\omega)$ can be obtained from the Kramers–Kronig relations in Eq. (3).

The real part of the dielectric function gives information about the refractive index of any material under investigation while imaginary part explains the absorption of light. The calculated imaginary ($\varepsilon_2$) and the real ($\varepsilon_1$) parts of the dielectric functions as a function of the photon energy are shown in Fig. 4(a)–(b) in the energy range of 0–20 eV. Although it has been established that $Sb_2S_3$ semiconductor has orthorhombic symmetry and this symmetry has three independent components of dielectric function, for this work we only consider polarization along [0 0 1] direction.

$$\varepsilon_1(\omega) = 1 + \left(\frac{2}{\pi}\right) \int_0^\infty d\omega' \frac{\omega'^2 \varepsilon_2(\omega')}{\omega'^2 - \omega^2} \quad (3)$$

The static dielectric constant, $\varepsilon_1(0)$ is the real part of dielectric constant at zero energy. These parameters were analyzed for $Sb_2S_3$ thin films as can be seen in Fig. 4(a). Table 2 shows an illustration of the static dielectric constant for different slabs. From the results, it is noticed that the value of static dielectric constant increases as the thin film thickness increases. Conversely, these are also important parameters that could be also used to obtain the energy band gap values of $Sb_2S_3$ thin films via Penn Model relation [64]. Using plasma energy $\hbar\omega_p$ and the value of $\varepsilon_1(0)$, the value of the energy gap of the title material can be calculated by using Penn expression. Interestingly, it was also observed that $Sb_2S_3$ thin films possesses plasmonic behavior when the thickness of the film is greater than one slab (1 slab). This negative behavior of real part (plasmonic behavior) is another exciting feature to make $Sb_2S_3$ thin film suitable for many applications [65–67].

It has been established that the imaginary part of dielectric function is directly connected with the energy band structure. The edge of optical absorption (first critical point) occurs at about 0.562, 0.589, 0.608, 0.607, 0.606 eV for 1, 2, 4, 6 and 8 slabs. Hence, the calculated imaginary part of the dielectric function shows that the first critical peak point is related to the transition from the valence to the conduction band states corresponding to the fundamental bandgap. The results of imaginary part of dielectric function indicate that $Sb_2S_3$ thin films have

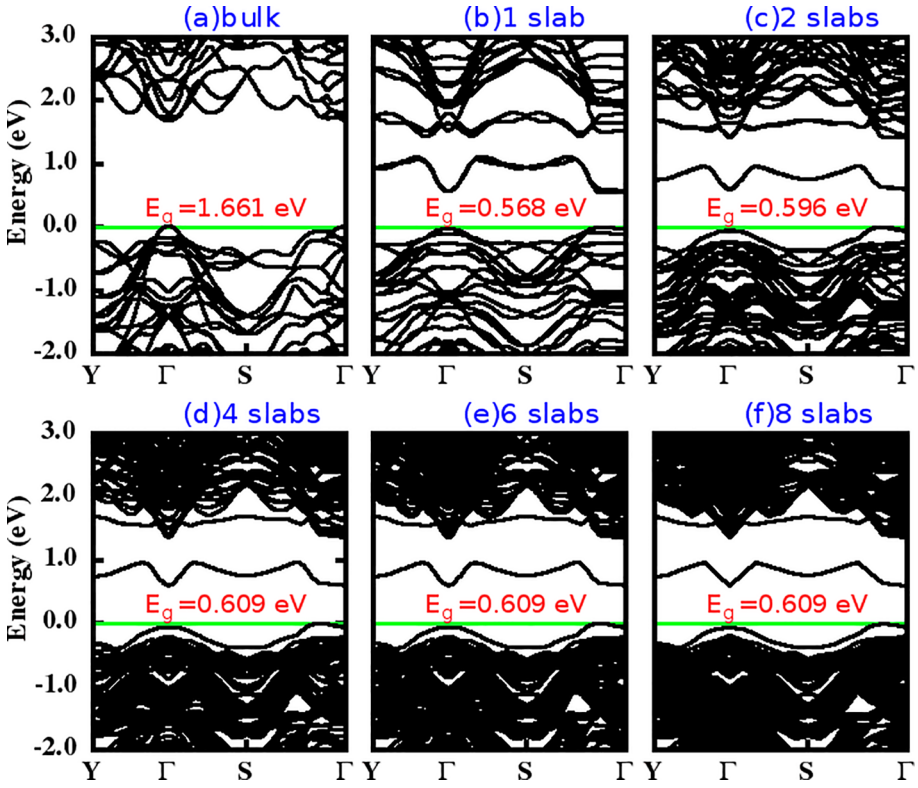


**Fig. 2.** Band structures of the bulk $Sb_2S_3$ (a) and $Sb_2S_3$ (0 0 1) thin films with five different thicknesses: 1 slab (b), 2 slabs (c), 3 slabs (d), 4 slabs (e), 5 slabs(f).

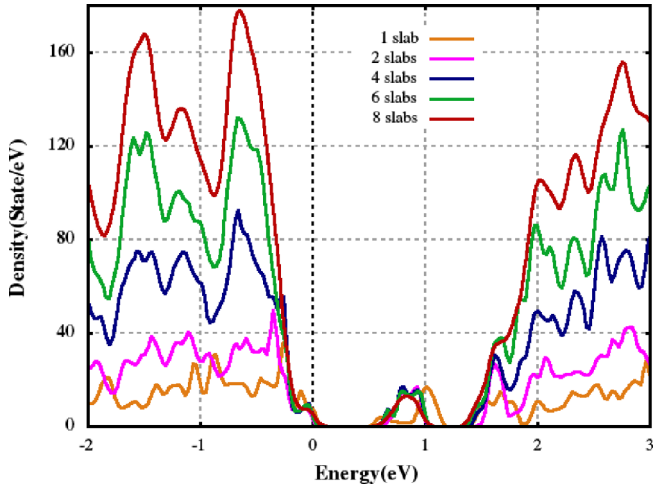


**Fig. 3.** Total density of states of the $Sb_2S_3$ (0 0 1) thin films with various thicknesses.

shown strong absorption in the visible light frequency, which depicts its suitability for optoelectronic applications. Apparently, due to crystallinity of the films, the optical absorption increases with the increase in the film thickness.

$$\alpha(\omega) = \frac{\omega}{c}\sqrt{2(\sqrt{\varepsilon_1^2(\omega) + \varepsilon_2^2(\omega)} - \varepsilon_1(\omega))} \tag{4}$$

$$n(\omega) = \sqrt{\left(\frac{\sqrt{\varepsilon_1^2(\omega) + \varepsilon_2^2(\omega)} + \varepsilon_1(\omega)}{2}\right)} \tag{5}$$

Using the knowledge of the complex dielectric constant, other optical parameters such as absorption coefficient, $\alpha(\omega)$ and refractive index, $n(\omega)$ can be determined. Fig. 4(c)–(d) shows the energy dependence of the absorption coefficient and refractive index. For photovoltaic applications, it is important to use a material with a suitable bandgap having large absorption coefficient [68]. When light rays strike the surface of a material, some part of its energy is reflected while some are transferred to the surface of the material. This transfer of energy to the surface is called absorption of light and it is represented in terms of absorption coefficient $\alpha(\omega)$. The graph of the absorption coefficient as a function of photon energy is presented in Fig. 4(c). From this graph, it is clear that $Sb_2S_3$ thin films shown good absorption coefficient values in the visible and ultraviolet wavelength range. Since $Sb_2S_3$ thin films show good absorption coefficients in the visible and ultraviolet-wavelength range for all thicknesses, it is anticipated that these films can be used asoptoelectronic devices. The curves of refractive index $n(\omega)$ in Fig. 4(d) are similar to the real part of dielectric function $\varepsilon_1(\omega)$ which is also in accordance with the established theory [69]. The values of static refraction index for different thickness of $Sb_2S_3$ (0 0 1) thin-film are given in Table 2. From the graph, we observed that the values of $n(\omega)$ in $Sb_2S_3$ (0 0 1) thin films are also influenced by the film thickness.

## Conclusion

In summary, the electronic and optical properties of $Sb_2S_3$ nano-thin films were studied by a highly accurate full-potential linearized augmented plane wave (FP-LAPW) approach based on DFT within EV-GGA exchange–correlation. The calculated values of indirect band gaps of $Sb_2S_3$ were found to be 0.568, 0.596 and 0.609 eV for 1, 2 and 4 slabs respectively. The bandgap values were found to be reduced when the thickness is increased. Although experimental research work at this scale is rare, this trend is consistent with experimental work where available. Optical properties including real and imaginary parts of the complex dielectric function, absorption coefficient, the refractive index were also investigated to understand the optical behavior of $Sb_2S_3$ nano-thin films. From the analysis of optical properties, it was clearly shown that $Sb_2S_3$ thin films have good optical absorption in the visible and ultraviolet wavelength range, it is, therefore, anticipated that these

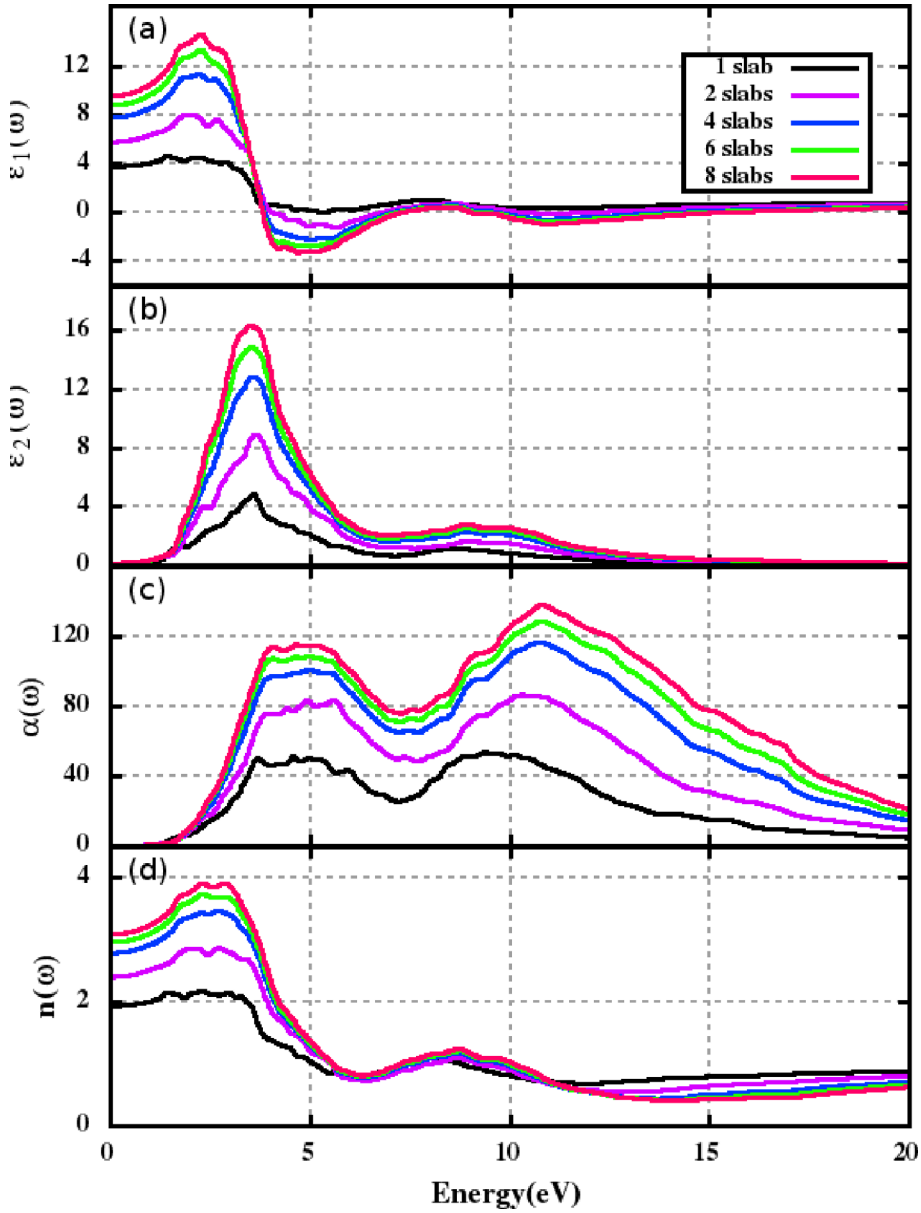


**Fig. 4.** (a) Real and (b) imaginary part of dielectric functions, (c) absorption coefficient and (d) refractive index for different slabs of $Sb_2S_3$ (0 0 1) thin films shown.

**Table 2**
Static dielectric, $\varepsilon_1(0)$ and Static refractive index, n(0) of $Sb_2S_3$ (0 0 1) thin films for different slabs.

| Thin film | | Static dielectric, $\varepsilon_1(0)$ | Static refractive index, n(0) |
|---|---|---|---|
| Number of slabs | 1 | 3.75 | 1.94 |
| | 2 | 5.80 | 2.41 |
| | 4 | 7.82 | 2.80 |
| | 6 | 8.83 | 2.97 |
| | 8 | 9.59 | 3.10 |

films can be used for versatile optoelectronic devices. However further investigations at experimental and theoretical levels with different techniques are recommended.

## Declaration of Competing Interest

The authors declare that they have no known competing financial interests or personal relationships that could have appeared to influence the work reported in this paper.

## Acknowledgement

This work was financially supported by the Universiti Teknologi Malaysia under the Research. University Grant (Vot No.: 12H46) and Ministry of Higher Education Malaysia.

## References

[1] Hussain NAA, Wan RAWN, Shaari SA. Antimony sulphide, an absorber layer for solar cell application. Appl Phys A 2016;122:1–7. https://doi.org/10.1007/s00339-015-9542-0.
[2] Gao C, Huang J, Li H, Sun K, Lai Y, Jia M, et al. Fabrication of Sb2S3 thin films by sputtering and post-annealing for solar cells. Ceram Int 2018. https://doi.org/10.1016/j.ceramint.2018.10.155.
[3] Lawal A. Theoretical study of structural, electronic and optical properties f bismuth-selenide, bismuth-telluride and antimony. Universiti Teknologi Malaysia; 2017.
[4] Romeo A, Terheggen M, Abou-Ras D, Bätzner DL, Haug F-J, Kälin M, et al. Development of thin-film Cu(In, Ga)Se2 and CdTe solar cells. Prog Photovoltaics Res Appl 2004;12:93–111. https://doi.org/10.1002/pip.527.
[5] Geisthardt RM, Topič M, Sites JR. Status and potential of CdTe solar-cell efficiency. IEEE J Photovoltaics 2015;5:1217–21. https://doi.org/10.1109/JPHOTOV.2015.2434594.
[6] Sasihithlu K, Dahan N, Greffet J. Light trapping in ultrathin CIGS solar cell with.

IEEE J Photovoltaics 2018;8:621–5. https://doi.org/10.1109/JPHOTOV.2018.2797522.
[7] Fthenakis VM. Overview of potential hazards. Elsevier 2012. p. 1083–96. doi:10.1016/B978-0-12-385934-1.00036-2.
[8] Wadia C, Alivisatos AP, Kammen DM. Materials availability expands the opportunity for large-scale photovoltaics deployment. Environ Sci Technol 2009;43:2072–7. https://doi.org/10.1021/es8019534.
[9] Munshi A, Sampath W. CdTe photovoltaics for sustainable electricity generation. J Electron Mater 2016:1–8. https://doi.org/10.1007/s11664-016-4484-7.
[10] Candelise C, Spiers JF, Gross RJK. Materials availability for thin film (TF) PV technologies development: a real concern? Renew Sustain Energy Rev 2011;15:4972–81. https://doi.org/10.1016/j.rser.2011.06.012.
[11] Efthimiopoulos I, Buchan C, Wang Y. Structural properties of Sb2S3 under pressure: evidence of an electronic topological transition. Sci Rep 2016;6:24246. https://doi.org/10.1038/srep24246.
[12] Zheng L, Jiang K, Huang J, Zhang Y, Bao B, Zhou X, et al. Solid-state nanocrystalline solar cells with an antimony sulfide absorber deposited by an in situ solid-gas reaction. J Mater Chem A 2017;5:4791–6. https://doi.org/10.1039/c7ta00291b.
[13] Radzwan A, Ahmed R, Shaari A, Ng YXYX, Lawal A. First-principles calculations of the stibnite at the level of modified Becke-Johnson exchange potential. Chin J Phys 2018;56:1331–44. https://doi.org/10.1016/J.CJPH.2018.03.005.
[14] Koc H, Mamedov AM, Deligoz E, Ozisik H. First principles prediction of the elastic, electronic, and optical properties of Sb2S3 and Sb2Se3 compounds. Solid State Sci 2012;14:1211–20. https://doi.org/10.1016/j.solidstatesciences.2012.06.003.
[15] Nair PK, González-Lua R, Calixto Rodríguez M, Capistrán Martínez J, GomezDaza O, Nair MTS. Antimony sulfide absorbers in solar cells. ECS Trans 2011;41:149–56. https://doi.org/10.1149/1.3628620.
[16] Ito S, Tsujimoto K, Nguyen D-C, Manabe K, Nishino H. Doping effects in Sb2S3 absorber for full-inorganic printed solar cells with 5.7% conversion efficiency. Int J Hydrogen Energy 2013;38:16749–54. https://doi.org/10.1016/J.IJHYDENE.2013.02.069.
[17] Choi YC, Lee DU, Noh JH, Kim EK, Il Seok S. Highly improved Sb2S3 sensitized-inorganic-organic heterojunction solar cells and quantification of traps by deep-level transient spectroscopy. Adv Funct Mater 2014;24:3587–92. https://doi.org/10.1002/adfm.201304238.
[18] Kriisa M, Krunks M, Oja Acik I, Kärber E, Mikli V. The effect of tartaric acid in the deposition of Sb2S3films by chemical spray pyrolysis. Mater Sci Semicond Process 2015;40:867–72. https://doi.org/10.1016/j.mssp.2015.07.049.
[19] Kondrotas R, Chen C, Tang J. Sb2S3 Solar Cells. Joule 2018;2:857–78. https://doi.org/10.1016/J.JOULE.2018.04.003.
[20] Bhandari GB, Subedi K, He Y, Jiang Z, Leopold M, Reilly N, et al. Thickness-controlled synthesis of colloidal PbS nanosheets and their thickness-dependent energy gaps. Chem Mater 2014;26:5433–6. https://doi.org/10.1021/cm502524z.
[21] Jena D, Konar A. Enhancement of carrier mobility in semiconductor nanostructures by dielectric engineering. Phys Rev Lett 2007;98:136805https://doi.org/10.1103/PhysRevLett. 98.136805.
[22] Chate PA, Sathe DJ, Lakde SD, Bhabad VD. A novel method for the deposition of polycrystalline Sb2S3 thin films. J Mater Sci: Mater Electron 2016;27:12599–603. https://doi.org/10.1007/s10854-016-5391-7.
[23] Qiao S, Liu J, Li Z, Wang S, Fu G. Sb2S3 thickness-dependent lateral photovoltaic effect and time response observed in glass/FTO/CdS/Sb2S3/Au structure. Opt Express 2017;25:19583–94. https://doi.org/10.1364/OE.25.019583.
[24] Lee YS, Bertoni M, Chan MK, Ceder G, Buonassisi T. Earth abundant materials for high efficiency heterojunction thin film solar cells. Conference Record of the IEEE Photovoltaic Specialists Conference, 2009, p. 002375–7. doi:10.1109/PVSC.2009.5411314.
[25] Ţigău N, Gheorghieş C, Rusu GI, Condurache-Bota S. The influence of the post-deposition treatment on some physical properties of Sb2S3 thin films. J Non-Cryst Solids 2005;351:987–92. https://doi.org/10.1016/j.jnoncrysol.2004.12.014.
[26] Salem AM, Selim MS. Structure and optical properties of chemically deposited Sb2S3 thin films. J Phys D Appl Phys 2001;34:12–7. https://doi.org/10.1088/0022-3727/34/1/303.
[27] Mak KF, Lee C, Hone J, Shan J, Heinz TF. Atomically thin MoS2: a new direct-gap semiconductor. Phys Rev Lett 2010;105:136805https://doi.org/10.1103/PhysRevLett. 105.136805.
[28] Mane RS, Lokhande CD. Thickness-dependent properties of chemically deposited Sb2S3 thin films. Mater Chem Phys 2003;82:347–54. https://doi.org/10.1016/S0254-0584(03)00271-2.
[29] Cohen ML, Chelikowsky JR. Electronic structure and optical properties of semiconductors. Springer Science & Business Media; 2012.
[30] Sham LJ, Schlüter M. Density-functional theory of the energy gap. Phys Rev Lett 1983;51:1888–91. https://doi.org/10.1103/PhysRevLett. 51.1888.
[31] Xiao H, Tahir-Kheli J, Goddard WA. Accurate band gaps for semiconductors from density functional theory. J Phys Chem Lett 2011;2:212–7. https://doi.org/10.1021/jz101565j.
[32] Demján T, Vörös M, Palummo M, Gali A. Electronic and optical properties of pure and modified diamondoids studied by many-body perturbation theory and time-dependent density functional theory. J Chem Phys 2014;141:064308https://doi.org/10.1063/1.4891930.
[33] Crowley J, Tahir-Kheli J, Goddard WA. Accurate Ab initio quantum mechanics simulations of Bi2Se3 and Bi2Te3 topological insulator surfaces. J Phys Chem Lett 2015;6:3792–6. https://doi.org/10.1021/acs.jpclett.5b01586.
[34] Baldini E, Chiodo L, Dominguez A, Palummo M, Moser S, Yazdi-Rizi M, et al. Strongly bound excitons in anatase TiO2 single crystals and nanoparticles. Nat Commun 2017;8:13. https://doi.org/10.1038/s41467-017-00016-6.
[35] Jin W, Yeh P-C, Zaki N, Zhang D, Sadowski JT, Al-Mahboob A, et al. Direct measurement of the thickness-dependent electronic band structure of MoS 2 using angle-resolved photoemission spectroscopy. Phys Rev Lett 2013;111:106801https://doi.org/10.1103/PhysRevLett. 111.106801.
[36] Dashora A, Ahuja U, Venugopalan K. Electronic and optical properties of MoS2 (0001) thin films: feasibility for solar cells. Comput Mater Sci 2013;69:216–21. https://doi.org/10.1016/j.commatsci.2012.11.062.
[37] Ye M, Winslow D, Zhang D, Pandey R, Yap Y. Recent advancement on the optical properties of two-dimensional molybdenum disulfide (MoS2) thin films. Photonics 2015;2:288–307. https://doi.org/10.3390/photonics2010288.
[38] Wang LP, De Han P, Zhang ZX, Zhang CL, Xu BS. Effects of thickness on the structural, electronic, and optical properties of MgF2 thin films: the first-principles study. Comput Mater Sci 2013;77:281–5. https://doi.org/10.1016/j.commatsci.2013.04.031.
[39] Kuc A, Zibouche N, Heine T. Influence of quantum confinement on the electronic structure of the transition metal sulfide TS2. Phys Rev B 2011;83:245213https://doi.org/10.1103/PhysRevB.83.245213.
[40] Ben Nasr T, Maghraoui-Meherzi H, Ben Abdallah H, Bennaceur R. Electronic structure and optical properties of Sb2S3 crystal. Phys B 2011;406:287–92. https://doi.org/10.1016/j.physb.2010.10.070.
[41] Chen J hua, Long X hao, Zhao C hua, Kang D, Guo J. DFT calculation on relaxation and electronic structure of sulfide minerals surfaces in presence of H2O molecule. J Central S Univers 2014;21:3945–54. https://doi.org/10.1007/s11771-014-2382-9.
[42] Radzwan A, Ahmed R, Shaari A, Lawal A, Xuan Ng Ying. First-principles calculations of antimony sulphide Sb2S3. Malaysian J Fundam Appl Sci 2017;89:18–21. https://doi.org/10.11113/mjfas.v13n3.598.
[43] Ben Nasr T, Maghraoui-Meherzi H, Kamoun-Turki N. First-principles study of electronic, thermoelectric and thermal properties of Sb2S3. J Alloy Compd 2016;663:123–7. https://doi.org/10.1016/j.jallcom.2015.12.093.
[44] Lakhdar MH, Ouni B, Amlouk M. Thickness effect on the structural and optical constants of stibnite thin films prepared by sulfidation annealing of antimony films. Optik 2014;125:2295–301. https://doi.org/10.1016/j.ijleo.2013.10.114.
[45] Engel E, Vosko SH. Exact exchange-only potentials and the virial relation as microscopic criteria for generalized gradient approximations. Phys Rev B 1993;47:13164–74. https://doi.org/10.1103/PhysRevB.47.13164.
[46] Blaha P, Schwarz K, Madsen G. WIEN2K, An Augmented Plane Wave+ Local Orbitals Program for Calculating Crystal Properties. 2001.
[47] Schwarz K. DFT calculations of solids with LAPW and WIEN2k. J Solid State Chem 2003;176:319–28. https://doi.org/10.1016/S0022-4596(03)00213-5.
[48] Khan W, Goumri-Said S. Engel-Vosko generalized gradient approximation within DFT investigations of optoelectronic and thermoelectric properties of copper thioantimonates(III) and thioarsenate(III) for solar-energy conversion. Phys Status Solidi (B) 2016;253:583–90. https://doi.org/10.1002/pssb.201552435.
[49] Benmessabih T, Amrani B, El Haj Hassan F, Hamdache F, Zoaeter M. Computational study of AgCl and AgBr semiconductors. Phys B 2007;392:309–17. https://doi.org/10.1016/j.physb.2006.11.046.
[50] Muhammad N, Khan A, Haidar Khan S, Sajjaj Siraj M, Shah SSA, Murtaza G. Engel-Vosko GGA calculations of the structural, electronic and optical properties of LiYO2. Phys B 2017;521:62–8.
[51] Kyono A, Kimata M. Structural variations induced by difference of the inert pair effect in the stibnite-bismuthinite solid solution series (Sb, Bi)2S3. Am Mineral 2004;89:932–40. https://doi.org/10.2138/am-2004-0702.
[52] Zhou G, Wang D. Few-quintuple Bi2Te3 nanofilms as potential thermoelectric materials. Sci Rep 2015;5:8099. https://doi.org/10.1038/srep08099.
[53] Maassen J, Lundstrom M. A computational study of the thermoelectric performance of ultrathin Bi $_2$ Te $_3$ films. Appl Phys Lett 2013;102:093103https://doi.org/10.1063/1.4794534.
[54] Mahmoodi T. A DFT Study on (001) Thin Slabs of SrTiO3 and BaTiO3. Acta Phys Pol A 2015;127:1616–20. https://doi.org/10.12693/APhysPolA.127.1616.
[55] Aramberri H, Muñoz MC. Strain effects in topological insulators: topological order and the emergence of switchable topological interface states in Sb 2 Te 3/Bi 2 Te 3 heterojunctions. Phys Rev B 2017;95:205422https://doi.org/10.1103/PhysRevB.95.205422.
[56] Acosta CM, Lima MP, da Silva AJR, Fazzio A, Lewenkopf CH. Tight-binding model for the band dispersion in rhombohedral topological insulators over the whole Brillouin zone. Phys Rev B 2018;98:035106https://doi.org/10.1103/PhysRevB.98.035106.
[57] Weisbuch C, Vinter B. Quantum semiconductor structures: Fundamentals and applications vol. 5. Elsevier; 2014.
[58] Dai J, Zeng XC. Bilayer phosphorene: Effect of stacking order on bandgap and its potential applications in thin-film solar cells. J Phys Chem Lett 2014;5:1289–93. https://doi.org/10.1021/jz500409m.
[59] Gan ZX, Liu LZ, Wu HY, Hao YL, Shan Y, Wu XL, et al. Quantum confinement effects across two-dimensional planes in MoS2 quantum dots. Appl Phys Lett 2015;106:233113https://doi.org/10.1063/1.4922551.
[60] Zhang Y, Chang T, Zhou B, Cui Y, Yan H, Liu Z, et al. Direct observation of the transition from indirect to direct band gap in atomically-thin epitaxial MoSe2. Nat Nanotechnol 2014;9:111–5. https://doi.org/10.1038/nnano.2013.277.
[61] Radzwan A, Ahmed R, Shaari A, Lawal A. Ab initio calculations of antimony sulphide nanowire. Phys B 2019;557:17–22. https://doi.org/10.1016/J.PHYSB.2019.01.005.
[62] Singh J. optical properties of condensed matter. John Wiley & Sons; 2006. doi:10.3109/17453674.2010.524593.
[63] Subramanian MA, Li D, Duan N, Reisner BA, Sleight AW. High dielectric constant in ACu3Ti4O12 and ACu3Ti3FeO12 phases. J Solid State Chem 2000;151:323–5.
[64] Penn DR. Wave-number-dependent dielectric function of semiconductors. Phys Rev 1962;128:2093–7. https://doi.org/10.1103/PhysRev. 128.2093.

[65] Lawal A, Shaari A, Ahmed R, Jarkoni N. First-principles investigations of electron-hole inclusion effects on optoelectronic properties of Bi2Te3, a topological insulator for broadband photodetector. Phys B 2017;520:69–75. https://doi.org/10.1016/J.PHYSB.2017.05.048.
[66] Li Y, Engheta N. Supercoupling of surface waves with ε -near-zero metastructures. Phys Rev B 2014;90:201107https://doi.org/10.1103/PhysRevB.90.201107.
[67] Savoia S, Castaldi G, Galdi V, Alù A, Engheta N. PT -symmetry-induced wave confinement and guiding in ε -near-zero metamaterials. Phys Rev B 2015;91:115114https://doi.org/10.1103/PhysRevB.91.115114.
[68] Fahrenbruch A, Bube R. Fundamentals of solar cells: Photovoltaic solar energy conversion. Elsevier; 2012. doi: 10.1115/1.3267632.
[69] Fox M, Bertsch GF. Optical properties of solids. Am J Phys 2002;70:1269–70. https://doi.org/10.1119/1.1691372.